Available online at www.sciencedirect.com
ScienceDirect
Ceramics International 36 (2010) 653–659
CERAMICS INTERNATIONAL
www.elsevier.com/locate/ceramint

The effects of templating synthesis procedures on the microstructure of Yttria Stabilised Zirconia (YSZ) and NiO/YSZ templated thin films

Anna Lashtabeg *, John L. Bradley, Guillaume Vives, John Drennan

ARC Centre of Excellence for Functional Nanomaterials, Australian Institute for Bioengineering and Nanotechnology (AIBN), University of Queensland, St. Lucia, QLD 4072, Australia

Received 16 May 2009; received in revised form 13 June 2009; accepted 30 September 2009
Available online 4 November 2009

Abstract

The microstructure of the electrodes, in particular the anode, is of vast importance in the present stage of Solid Oxide Fuel Cell (SOFC) development. Templating methods provide well ordered, inverse opal, macroporous structures for small quantities of powder, scaling up the procedure to produce commercial quantities of powder remains a challenge. This study examined different synthesis conditions for producing larger amounts of high quality YSZ and NiO/YSZ electrodes using the templating technique and the effects of these on microstructure. The study revealed that as the quantity of the polystyrene (PS) spheres for the template is increased the microstructure quality is reduced, due to increasing difficulty in homogeneous permeation of the template. Thus the optimisation of the ratio of PS spheres to powder is of great importance and in this study was found to be around 2:1, however the addition of NiO has additional effects on the microstructure.

Keywords: Yttria Stabilised Zirconia (YSZ); SOFC anode; Microstructure; Templating; Polystyrene spheres; Humidity; Thin film

1. Introduction

The targeted control of porosity has been studied and used in a wide range of applications such as membranes for separation and purification, high surface area adsorbants [1], supports for sensors and catalyst [2], photonic crystals [3–5] and electrodes for fuel cells [6–10].

Hard templating methods using colloid crystalline templates [11], such as polystyrene or silica spheres, to produce three-dimensional ordered macroporous (3DOM) materials are becoming an increasingly popular way to synthesise a wide range of materials and have been extensively studied for materials such as silica [12], metals [13], semiconductors [3], metal oxides [14–17], carbon [18] and polymers [19,20].

Templating particles range in size from nanometres to micrometres and self-assemble in the correct synthesis conditions into cubic close packed arrays. Once infiltrated with precursor solution and then either chemically or thermally removed, the long range periodic ordering of spheres is replicated in a solid, inverse opal matrix, yielding materials with ordered pores. An advantage of the template method is that the dimensions of the pores in the final material are set by the size of the template, thus the microstructure can be readily tailored, with both the final porosity and the surface area determined by the size of the template particles.

Yttria Stabilised Zirconia (YSZ) is commonly used as an oxygen sensor and an oxygen pump in automotive and industrial applications, and is the choice electrolyte for commercial Solid Oxide Fuel Cell (SOFC) technology. YSZ is also a major component of the SOFC anode where it is typically mixed with 50 vol% NiO and then reduced at operating conditions to create a varyingly porous Ni/YSZ cermet electrode. The porosity is important in two regards: efficient gas transport through the electrode and high surface area for catalytic reactions. Thus optimising pore size and size distribution in the anode is necessary for achieving fast gas transport to and from all catalytically active sites, and will result in optimum electrochemical performance and even distribution of fuel.

To date the electrode porosity is only loosely controlled by the powder morphology, sintering conditions and the addition of pore formers, such as graphite powders [21]. In

* Corresponding author.
E-mail address: a.lashtabeg@uq.edu.au (A. Lashtabeg).

0272-8842/$36.00
doi:10.1016/j.ceramint.2009.10.009

the SOFC anode further porosity is introduced with the change in Ni fraction due to NiO reduction to Ni metal. Whereas templating methods for SOFC electrode optimisation have been attempted for a limited number of materials, YSZ [10,14,17], $Ce_{0.9}Gd_{0.1}O_{1.95}$ [6], $Sm_{0.5}Sr_{0.5}CoO_3$ [6], $La_{0.75}Sr_{0.25}Cr_{0.5}Mn_{0.5}O_{3-\delta}$ [8,9], $Ba_{0.5}Sr_{0.5}Co_{0.8}Fe_{0.2}O_{3-\delta}$ [8,9].

When fabricating electrodes for fuel cell testing, three approaches are used for producing templated structures. In the first approach the template is deposited onto the electrolyte directly and infiltrated with the electrode precursor solution [17] and sintered at high temperature to produce the electrode as a thin film. The second approach is to pre-fabricate the templated electrode as loose powder by infiltration, and then press and sinter the electrode onto the substrate or into a pellet for testing. The infiltration method produces better ordering and more precise replication of the templated matrix, however additional handling of the powder in the pre-fabrication stage tends to damage the templated powder.

The third approach is to use nano- or submicron powder mixed with the template and sinter it into a pellet or directly onto the electrolyte. In this non-infiltration method, the ordering is diminished, and large degree of randomisation of pores is present.

All of the groups that synthesised testable quantities of powder did so at the expense of microstructure. For example, Ruiz-Morales et al. [8,9], used a mixture of YSZ powder, monodisperse 500 nm PMMA microspheres and polyvinyl alcohol to prepare well ordered YSZ pores, and subsequently electrodes at fabrication temperatures up to 1200 °C. Although they found superior fuel cell performance compared to non-optimised structures, as the microspheres were not infiltrated with a solution prior to sintering a certain degree of randomness remained in the ordering of the pores. This may account for the structural collapse at 1200 °C and by 1400 °C no regular structure was observed. In contrast, Lashtabeg et al. [17] found that the infiltration method produced highly ordered structures which remained stable to 1400 °C during sintering, yet no one to date has addressed an issue of scaling up the procedure for large scale powder production, which remains a challenge.

In our previous study [17] we demonstrated that a well studied templating technique can be used to synthesise well ordered highly porous structures for YSZ that are stable to 1400 °C, however the major challenge is to use this method to produce electrodes that can be sintered onto the electrolyte and tested in fuel cell conditions, i.e. bulk powder production for processing. In the previous study the electrode films showed cracking and domain formation, the occurrence of which was attributed to large shrinkage during the template and metal nitrate decomposition at 400–650 °C.

In this study we are looking at different approaches to produce a continuous and well structured electrode using both infiltration and mixing techniques and examining the effect on the microstructure. This study also aims to examine the effect on microstructure of the addition of NiO to form a NiO/YSZ cermet. In addition we are looking to control the drying and decomposition conditions in order to use the infiltration technique to produce an electrode that can be directly sintered onto the electrolyte. The success would have wide reaching implications for SOFC technology if achieved in that the hard templating method would be a viable route to mass scale electrode manufacture.

2. Experimental

Three approaches to electrode production were examined:

1. A one step direct infiltration of commercially available polystyrene (PS) spheres deposited directly onto the electrolyte surface, followed by decomposition and sintering steps.
2. A two step process, involving the production of templated electrodes followed by screen printing of the modified powder onto the electrolyte.
3. A two step non-infiltration approach, involving the production of inks consisting of nano-powder, PS, solvents and binding agents, followed by screen printing onto an electrolyte and sintering.

2.1. Hard templating by infiltration directly onto the electrolyte

A 2.5% solution of monodisperse (1 ± 0.05 μm) PS spheres (Fluka) in water was used as received to create the template. The PS spheres were added drop wise to an 8 mol% Yttria Stabilised Zirconia (8YSZ) solid electrolyte plate, density >99%. The spheres were left to self-assemble into a close packed structure by drying in air at ambient temperature, before the addition of a subsequent droplet of PS spheres, thus eventually producing a self-organised PS template to serve as three-dimensional scaffolding.

Due to the small size of PS spheres high permeation of the voids was achieved by a drop wise addition of reagent quality $ZrO(NO_3)_2{\cdot}xH_2O$ (Sigma–Aldrich) and $Y(NO_3)_3{\cdot}6H_2O$ (Sigma–Aldrich) dissolved in methanol, in the correct stoichiometric ratios to form the 4 mol% Yttria Stabilised Zirconia (4YSZ) backbone. It was found that methanol allows a better surface wetting than water or ethanol, and causes the least disruption to the polystyrene template during infiltration.

The ratio of PS spheres volume and 4YSZ volume was kept at 76:24, corresponding to the free volume between the spheres in the fcc packing arrangement. An exact amount of 4YSZ precursor solution was added drop wise to the PS template and after 1–2 drops the solvent was allowed to evaporate in air at room temperature before further addition of the solution. After the final addition of the solution the 'wet' samples were subjected to a series of thermal and humidity treatments in order to dry the coatings. A tube furnace with flowing humidified air was used to control the temperature and the humidity. The ramp rate to the drying temperature was kept at <1 °C/min by the fine control of the furnace controller PID parameters.

The final decomposition and sintering were carried out at 650–1000 °C with heating and cooling ramp rates of 5 °C/min and dwell times of 1 h.

2.2. Pre-fabrication of powder by infiltration method and screen printing

Dry monodisperse 1 μm polystyrene spheres (Soken Chemicals) were dispersed in water using an ultrasonic bath, followed by centrifuging at 2500 rpm for 20 min, and subsequent drying at 50 °C. These were infiltrated with a $ZrO(NO_3)_2{\cdot}xH_2O$, $Y(NO_3)_3{\cdot}6H_2O$ and $Ni(NO_3)_3{\cdot}6H_2O$ (Sigma–Aldrich) dissolved in 1:1 mixture of water and ethanol. For samples incorporating NiO, the loading of NiO was kept to 50 vol% mixed with the YSZ precursor solution, in line with the ideal anode loading. The weight ratio of PS to YSZ equivalent was varied, at 4:1, 3:1 and 2:1 in order to identify the optimum microstructure.

The solvent was evaporated at 50 °C for 12 h, followed by drying at 100 °C for 3 h, and sintering at 1000 °C for 5 h, with heating and cooling ramp rates of 5 °C/min. Additional sintering was performed on powder at 1300 °C to fortify the structure prior to mixing it into slurry using cellulose binder, diethylene glycol monoethyl ether, water and isopropanol as solvents. The slurry was then screen printed onto masked 15 mm wide 8 mol% YSZ electrolyte disks (Pi-KEM) to form 10 mm × 10 mm electrodes.

2.3. Nano-powder mixture with PS and screen printing

Dry monodisperse 1 μm polystyrene spheres (Soken Chemicals) and YSZ nano-powder (Sigma–Aldrich) were mixed together in a weight ratio of 3:1 (PS:YSZ) with water ethanol as solvent and 5 wt% PVA as binder to form a slurry. The slurry was then screen printed onto 15 mm wide 8 mol% YSZ electrolyte disks (Pi-KEM), masked to form 10 mm × 10 mm electrodes. The electrodes were then dried at 40 °C prior to sintering at 1350 °C, with a heating ramp rate of 1–2 °C/min and 10 °C/min cooling rate.

2.4. Instrumentation

Scanning electron microscope images were obtained using the JEOL 6400 operated at 5–10 keV to minimise specimen charging. The samples were coated with a 30 nm layer of platinum using EIKO IB-5 Sputter Coater to further reduce sample charging. XRD was performed using a Bruker D8 Advance X-ray diffractometer with CuKα radiation, with 2θ scanning range of 5–90° at intervals of 0.02°, and with stepping time of 1.2 s. Image J software was used to calculate surface areas and lengths of coatings and cracks.

3. Results

3.1. Infiltration directly onto the electrode

Using the standard infiltration procedure directly on the surface of the electrolyte as described in this paper and elsewhere [17] allows the production of 20 mg of powder, with 50–100 μm 'domains' formed after shrinkage. The microstructure of such powder is highly ordered and represents a true inverse opal template, seen in Fig. 1. Such small quantities of powder are unsuitable for large scale SOFC electrode production and the scale up of powder production is needed.

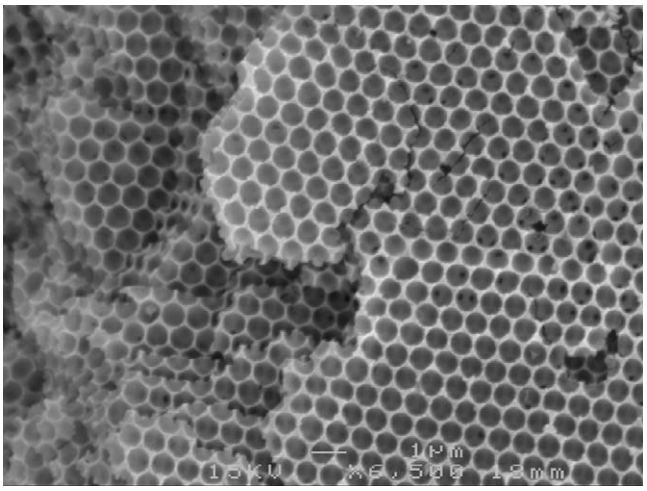

Fig. 1. Inverse opal structure produced using hard templating and infiltration technique [17].

The ability to form the templated electrodes directly onto the electrolyte substrate and sinter in one step, giving a highly ordered structure, would be an ideal procedure for mass scale production. However, the main issue of cracking and domain formation has to be overcome. In an attempt to control the shrinkage rate, the humidity and drying temperature were varied and the average domain size calculated.

Fig. 2 shows the cracking of the template due to shrinkage forming domains separated by cracks. Although initially believed to occur due to shrinkage during the decomposition and sintering stage, Fig. 3 shows that the cracking of films occurs during the initial drying stage at room temperature, prior to heat treatment or sintering. We have found that water, ethanol, methanol or a mixture of these did not have a significant effect on cracking, however methanol was found to cause the least amount of disturbance to the template. The

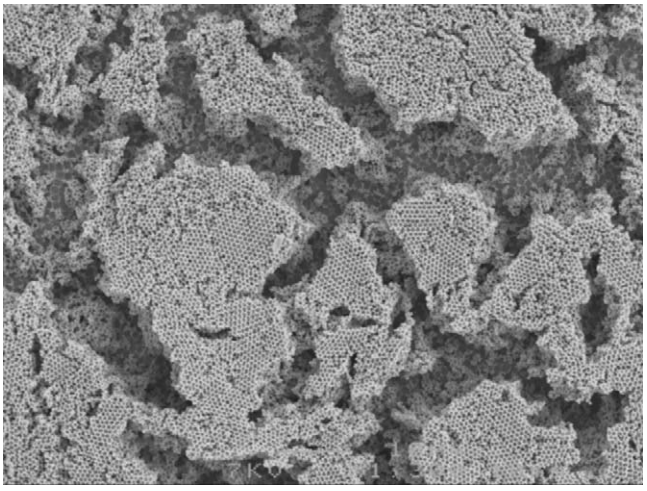

Fig. 2. 4YSZ sintered at 800 °C showing 'domains' and cracking of porous templates caused by shrinkage during the drying stage.

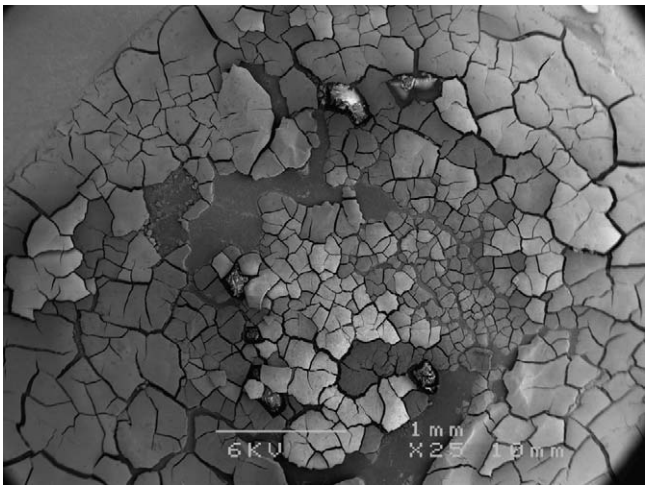

Fig. 3. PS template and infiltrate solution dried at room temperature (21 °C) in air.

infiltration step causes large disturbance to the three-dimensional PS template, and rapid drying exacerbates the problem.

In order to reduce the drying rate, the humidity and drying temperatures were varied in a tube furnace using flowing humidified air at a rate of 10 ml/min. The ramp rate to the drying temperature was kept at <1 °C/min to avoid rapid drying and shrinkage.

Fig. 4(a) shows the effect of gas humidification on the average size of the 'domain' units. The size of the domains and the distance between adjacent fragments indicate the degree of fragmentation. From Fig. 4 it can be seen that humidity is an important factor in producing a continuous electrode layer without fragmentation needed for SOFC application. Increasing the humidity has an effect of slowing the drying rate and thus the shrinkage rate. The smallest degree of fragmentation occurs at >70% humidification and it can be concluded that high humidity is necessary for bulk contraction of the film in order to maintain the template microstructure. At lower humidification the drying is inhomogeneous and cracking and islandisation increase accordingly, and can be understood in terms of the rapid drying of the surface of the film compared to bulk de-humidification in the dry atmosphere. Increasing the humidification of the atmosphere thus decreases the moisture gradient across the film resulting in an increase in homogeneous drying rate and larger domain size.

Fig. 4(b) shows the effect of drying temperature on the degree of fragmentation, and from this it can be seen that increasing the drying temperature at high humidity also decreases the degree of fragmentation. However it was expected that the lower temperature should increase the drying time, and thus produce the opposite effect, thus highlighting the higher importance of humidity on the electrode microstructure. The higher drying temperature leads to an increase in vapour pressure above the film surface resulting in homogeneous drying of the film as the surface dries at a similar rate to the bulk.

3.2. Pre-fabrication of powder by infiltration and screen printing

Increasing powder production to 300 mg allows the pre-fabrication of the electrodes prior to screen printing. The

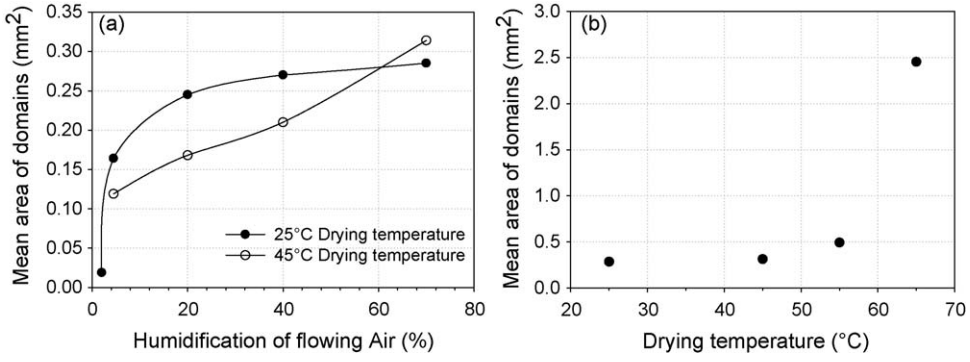

Fig. 4. The effects of (a) humidity and (b) drying temperature at constant humidity of 70% on the mean area of domains in the YSZ film.

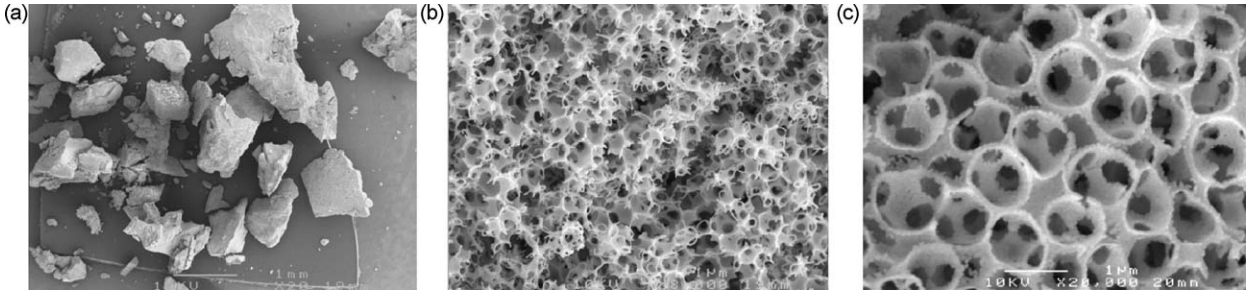

Fig. 5. YSZ from 4:1 wt ratio of PS to YSZ sintered at 1000 °C.

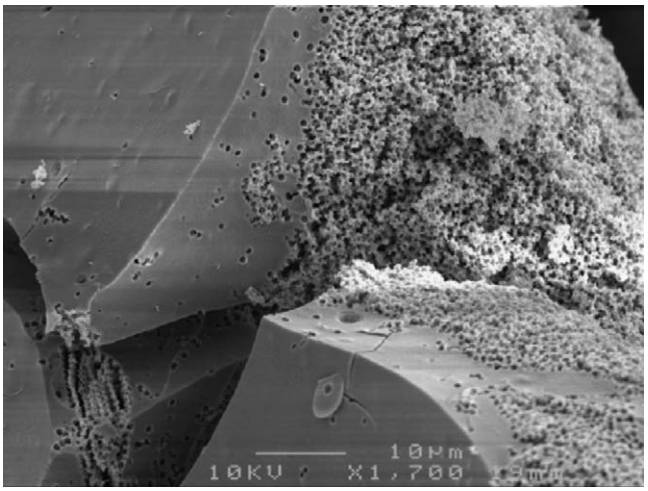

Fig. 6. Incomplete permeation of PS spheres due to excess solution.

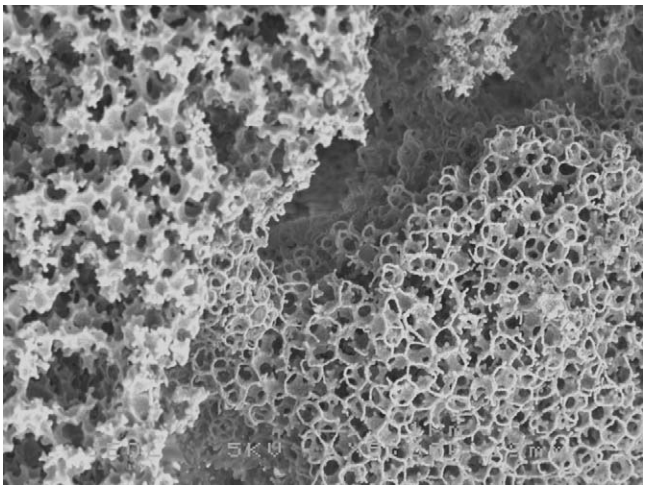

Fig. 8. Microstructure of YSZ produced from the 3:1 ratio of PS spheres to YSZ equivalent.

infiltration of large quantities of PS spheres, as described in Section 2, produced powder consisting of 1–10 mm ''domains'' (Fig. 5(a)). However, as can be seen in Figs. 5–7 the quality of the microstructure is reduced.

The ratio of metal nitrate solution to polystyrene spheres must be optimised, as too little infiltrating solution will produce weaker walls and structural collapse on sintering, as seen in the 4:1 ratio in Fig. 5, whereas too much infiltrate will produce incomplete permeation and dense regions of YSZ, such as the ones seen in Fig. 6. The regions of optimum PS to YSZ ratio produced highly ordered structures within regions of less ordered microstructure (Fig. 7).

Changing the weight ratio to 2:1 of PS sphere to YSZ equivalent, improves the microstructure by producing stronger walls and increasing occurrence of regular pores from the template. In addition the surface area of the samples sintered at 1200 °C increased from 10 m^2/g for the 4:1 ratio, to >20 m^2/g for the 2:1 ratio.

In the region of intermediate weight ratio of 3:1 of PS spheres to YSZ equivalent, the microstructure is non-

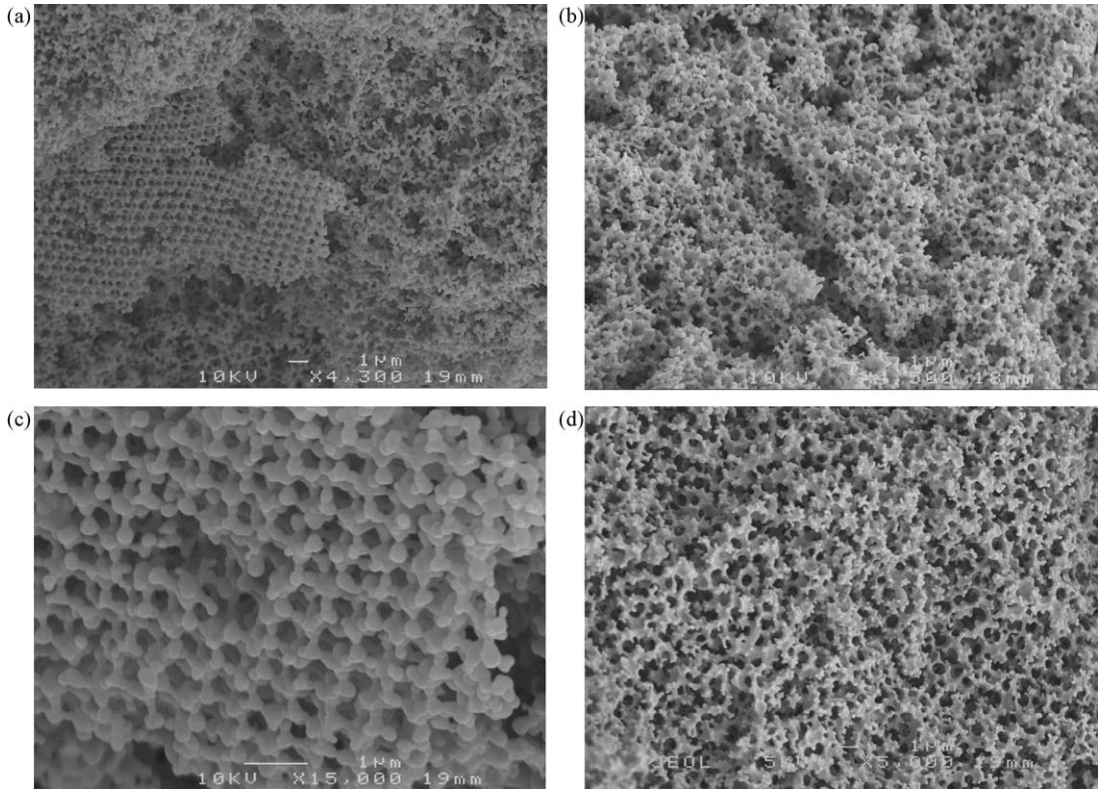

Fig. 7. (a–c) YSZ powder produced from 4:1 wt ratio of PS to YSZ equivalent and sintered at 1200 °C, (d) YSZ powder produced from 2:1 wt ratio of PS to YSZ equivalent and sintered at 1200 °C.

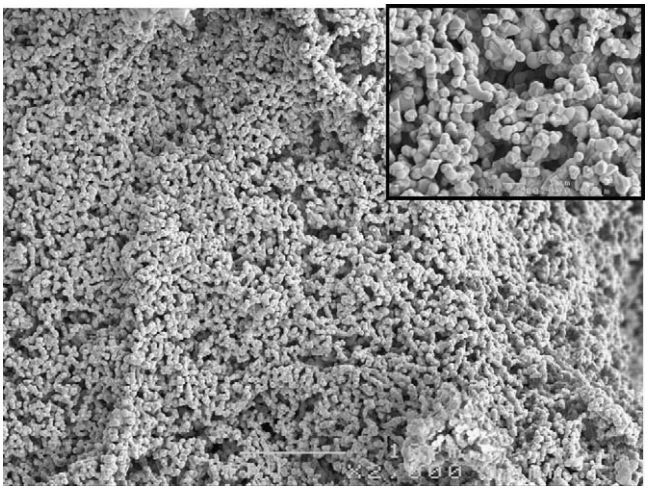

Fig. 9. 50 vol% NiO/YSZ using PS:NiO/YSZ of 2:1 and sintering temperature of 1300 °C.

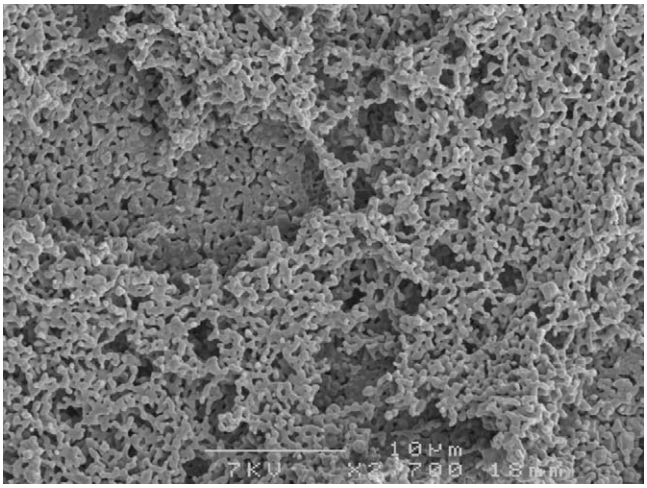

Fig. 10. Microstructure of YSZ nano-powder thin film produced from 3:1 mix of YSZ and PS spheres followed by screen printing.

homogeneous, composed of both poor permeation and high permeation regions (Fig. 8).

In addition, when scaling up the infiltration templating technique, experimental factors will have a profound effect on the microstructure of the final powder. This relates directly to the disturbance of the template. Although the centrifuging will form a compact layer of self-assembled PS spheres the addition of highly polar solvent will disturb the assembly of spheres, producing a more randomised distribution of pores, similar to the present use of pore formers. In order to minimise the disturbance, larger dilutions of nitrates are needed using solvents such as ethanol and methanol.

The addition of NiO invariably changes the microstructure in the cermet NiO/YSZ, where the inverse opal structure has not been achieved due to the segregation of NiO and YSZ phases into distinct nanoparticles (Fig. 9). The optimum ratio of PS to YSZ of 2:1 does not apply to NiO and further work is needed to find the optimum condition for incorporating NiO into the microstructure.

Thus the challenge to date remains: to replicate this microstructure on a larger scale throughout the electrode, and find the most suitable route to powder production which gives the largest degree of morphology homogeneity. However the advantage of this procedure is the possibility of controlling microstructures not only by selecting the size and type of template, but also by the synthesis procedure itself.

3.3. Non-infiltration mixing of nano-powder and PS and screen printing

This route is the most commonly used for producing highly porous electrodes for testing where monodisperse spheres serve as pore formers. It is therefore not a true hard templating technique and does not produce a true inverse opal microstructure (Fig. 10). Mixing the PS spheres in the ratio of 3:1 with YSZ nano-powder produced a microstructure with irregular porosity, with randomised pore size, pore distribution and YSZ particle size. This technique is the least effective at controlling porosity.

4. Conclusions

A range of microstructures have been synthesised by changing the synthesis procedure whilst using the same 1 μm template of polystyrene spheres and either metal nitrate precursors or nano-powder.

In this paper we proposed different approaches to producing large quantities of powder and examined the effect on the microstructure of the final electrodes. It was found that in scaling up the microstructure deteriorates either during synthesis or post-synthesis powder treatment. It may be possible to synthesise thin films directly onto the substrate or support using the templating technique, however the issue of film cracking during the drying stage must be addressed. In this study we found that increasing the drying temperature and humidity decreases the number and size of cracks and in a pressurised, humidity-controlled drying oven the film may show further improvement.

The study demonstrated that inverse opal templated porosity is only maintained for small quantities of powder; however the ability to modify the microstructure not solely by templating but also by additional synthesis and processing allows tailoring of materials' properties to a specific task for a wide range of applications.

Acknowledgements

The authors thank Ceramic Fuel Cells Limited (Melbourne) and The Centre for Microscopy and Microanalysis (CMM) at the University of Queensland for use of facilities and the Australian Institute for Bioengineering and Nanotechnology (AIBN) for financial support.

References

[1] S. Madhavi, C. Ferraris, T.J. White, Journal of Solid State Chemistry 178 (2005) 2838.
[2] C. Wang, A. Geng, Y. Guo, S. Jiang, X. Qu, L. Li, Journal of Colloid and Interface Science 301 (2006) 236.

[3] N.Y. Yurii, A. Vlasov, D.J. Norris, Advanced Materials 11 (1999) 165.
[4] S.H. Im, Y.T. Lim, D.J. Suh, O.O. Park, Advanced Materials 14 (2002) 1367.
[5] J.E.G.J. Wijnhoven, W.L. Vos, Science 281 (1998) 802.
[6] Y. Zhang, S. Zha, M. Liu, Advanced Materials 17 (2005) 487.
[7] F. Chen, C. Xia, M. Liu, Chemistry Letters 30 (2001) 1032.
[8] J.C. Ruiz-Morales, J. Canales-Vazquez, J. Pena-Martinez, D.M. Lopez, P. Nunez, Electrochimica Acta 52 (2006) 278.
[9] J.C. Ruiz-Morales, J. Canales-Vazquez, J. Pena-Martinez, D. Marrero-Lopez, J.T.S. Irvine, P. Nunez, Journal of Materials Chemistry 16 (2006) 540.
[10] M. Boaro, J.M. Vohs, R.J. Gorte, Journal of the American Ceramic Society 86 (2003) 395.
[11] O.D. Velev, E.W. Kaler, Advanced Materials 12 (2000) 531.
[12] O.D. Velev, T.A. Jede, R.F. Lobo, A.M. Lenhoff, Nature 389 (1997) 447.
[13] O.D. Velev, P.M. Tessier, A.M. Lenhoff, E.W. Kaler, Nature 401 (1999) 548.
[14] B.T. Holland, C.F. Blanford, T. Do, A. Stein, Chemistry of Materials 11 (1999) 795.
[15] P. Yang, T. Deng, D. Zhao, P. Feng, D. Pine, B.F. Chmelka, G.M. Whitesides, G.D. Stucky, Science 282 (1998) 2244.
[16] B.T. Holland, C.F. Blanford, A. Stein, Science 281 (1998) 538.
[17] A. Lashtabeg, J. Drennan, R. Knibbe, J.L. Bradley, G.Q. Lu, Microporous and Mesoporous Materials 117 (2009) 395.
[18] A.A. Zakhidov, R.H. Baughman, Z. Iqbal, C. Cui, I. Khayrullin, S.O. Dantas, J. Marti, V.G. Ralchenko, Science 282 (1998) 897.
[19] S.A. Johnson, P.J. Ollivier, T.E. Mallouk, Science 283 (1999) 963.
[20] Y.X. Sang Hyun Park, Advanced Materials 10 (1998) 1045.
[21] S.P. Jiang, P.J. Callus, S.P.S. Badwal, Solid State Ionics 132 (2000) 1.